

In-context Demonstration Matters: On Prompt Optimization for Pseudo-Supervision Refinement

Zhen-Yu Zhang

Center for Advanced Intelligence Project, RIKEN

ZHEN-YU.ZHANG@RIKEN.JP

Jiandong Zhang

Northeastern University

ZHANG.JIANDO@NORTHEASTERN.EDU

Huaxiu Yao

UNC-Chapel Hill

HUAXIU@CS.UNC.EDU

Gang Niu

Center for Advanced Intelligence Project, RIKEN

GANG.NIU@RIKEN.JP

Masashi Sugiyama

Center for Advanced Intelligence Project, RIKEN

SUGI@K.U-TOKYO.AC.JP

Graduate School of Frontier Sciences, The University of Tokyo

Abstract

Large language models (LLMs) have achieved great success across diverse tasks, and fine-tuning is sometimes needed to further enhance generation quality. Most existing methods rely on human supervision or parameter retraining, both of which are costly in terms of data collection and computational resources. To handle these challenges, a direct solution is to generate “high-confidence” data from unsupervised downstream tasks and use them for in-context prompting or prompt optimization to refine the pseudo-supervision. However, relying solely on such data may lead to *overfitting*. In this paper, we leverage the *in-context learning* (ICL) abilities of LLMs and propose a novel approach, *pseudo-supervised demonstrations aligned prompt optimization* (PAPO) algorithm, which jointly refines both the prompt and the overall pseudo-supervision. The proposed learning objective ensures that the optimized prompt guides the LLM to generate consistent responses for a given input when pseudo-supervised data from the downstream task are used as demonstrations, enabling refinement over the entire pseudo-supervision. The prompt is optimized by translating gradient signals into textual critiques, which serve as feedback to iteratively refine the prompt and model responses. Theoretical analysis in a simplified classification setting shows that the refined pseudo-supervision exhibits a geometric clustering structure, helping to mitigate overfitting. Experiments on question answering, natural language inference benchmarks, and a real-world molecule optimization task, show the effectiveness of the proposed algorithm.

1. Introduction

Large language models have shown impressive performance on various real-world tasks (Brown et al., 2020; Achiam et al., 2023; Yang et al., 2024). Since most LLMs are trained for general purpose use, fine-tuning is often necessary to enhance their performance on specific downstream applications. For instance, *reinforcement learning from human feedback* (RLHF) techniques align LLMs using human preference data (Ouyang et al., 2022; Rafailov et al., 2023). Despite their effectiveness, these approaches typically involve retraining, which can be time-consuming and limit the model’s responsiveness to rapidly changing data distributions and task requirements. Meanwhile, these methods require supervised data to update the model, while human feedback is hard to obtain in many real-world tasks. Therefore, it is important to design algorithms that *improve the generation quality of LLMs at test time using unsupervised data, without retraining the model parameters*.

Existing approaches relevant to this learning problem include *test-time alignment* and *self-refinement* strategies. However, current test-time alignment methods mostly consider the preference alignment task and heavily rely on human supervision, whereas self-refinement approaches typically require retraining

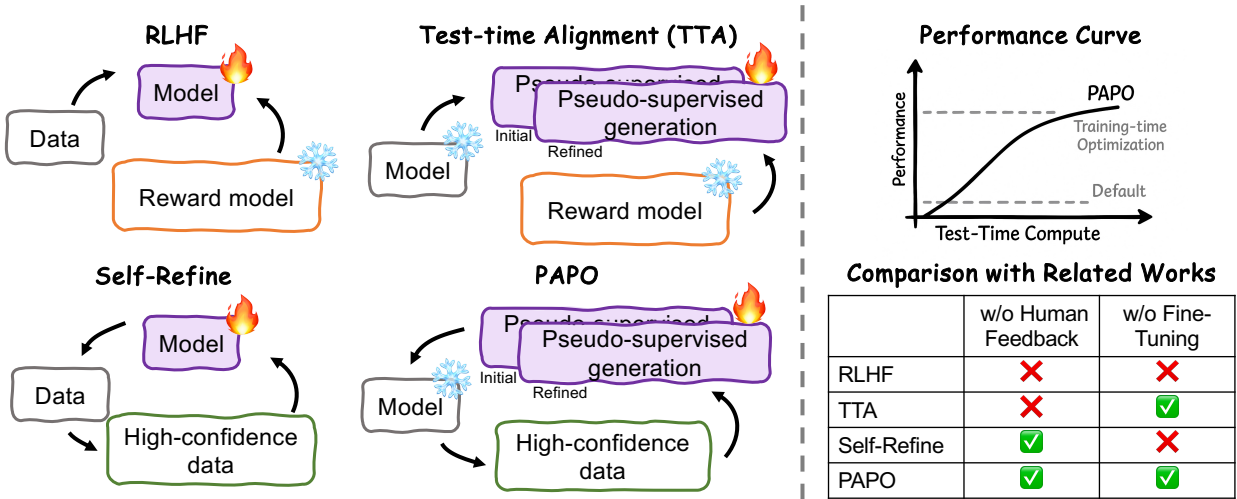


Figure 1: Comparison between training-time optimization (e.g., RLHF and Self-Refine) and test-time optimization with or without human supervision (e.g., Test-time Alignment and PAPO). PAPO enables test-time refinement without retraining model parameters or requiring human supervision.

model parameters, which can be computationally expensive. For instance, Best-of-N sampling is a typical test-time alignment method (Lightman et al., 2024; Zhang et al., 2024) that generates multiple candidate responses and selects the one with the highest score according to a reward model trained on human feedback. Although these methods are effective, their dependence on human supervision can limit generalization. To handle this challenge, self-refinement techniques (Huang et al., 2023; Wang et al., 2023; Sun et al., 2024) allow models to explore “high-confidence” self-generated responses and update themselves accordingly. Nevertheless, these methods require retraining of model parameters, resulting in substantial computational overhead.

To support test-time refinement without retraining model parameters, a feasible method is to first identify “high-confidence” pseudo-supervised data, which can be obtained either via the *chain-of-thought* (CoT) mechanism (Wei et al., 2022) or through scoring functions. Building on this, recent seminal works leverage these selected data as in-context demonstrations (Brown et al., 2020) to guide final predictions (Wan et al., 2023a,b; Guo et al., 2024; Li et al., 2024). While effective, these approaches depend heavily on the selected “high-confidence” data. In practice, over-reliance on such self-selected pseudo-supervised data may lead to *overfitting* (Bishop, 2006; Goodfellow et al., 2016). This may lead the model to reinforce biases present in these data, ultimately resulting in degraded performance.

In this paper, we explore the *in-context learning* (Brown et al., 2020) ability of LLMs for test-time refinement. ICL generates responses by conditioning on labeled demonstrations, and has been theoretically shown to perform equivalently to gradient descent under certain conditions, without updating model parameters (Bai et al., 2023). We incorporate pseudo-supervised data in the downstream task as demonstrations during prompt optimization to mitigate overfitting. This is achieved by regularizing the refined pseudo-supervised data to exhibit internal consistency: when used as in-context demonstrations, they should guide the model to produce aligned outputs, even when those demonstrations are not explicitly provided. Ideally, in a simplified classification setting, the empirical risk minimizer over any subset is expected to yield consistent pseudo-labels on the rest of the data after refinement. In other words, we propose encouraging a cluster structure in the refined pseudo-supervised data to mitigate overfitting, a well-established principle in semi-supervised learning and self-supervised learning (Chapelle et al., 2006; Belkin et al., 2006).

Building on this idea, we propose a novel test-time refinement algorithm, called *pseudo-supervised demonstrations aligned prompt optimization* (PAPO), which enhances generation quality without relying on human supervision or retraining model parameters, as illustrated in Figure 1. Specifically,

we integrate prompt optimization with the ICL capability of LLMs by iteratively identifying a set of “high-confidence” pseudo-labeled data, and then jointly refining the model’s generation and optimizing the prompt based on these examples. The learning objective is to minimize the loss on these “high-confidence” data, with the pseudo-supervised data serving as in-context demonstrations. We use TextGrad (Yuksekgonul et al., 2024) to optimize the prompt through gradient-based updates with textual feedback, similar to gradient descent. Theoretical analysis shows that, in the simplified setting of classification, the refined output exhibits a cluster structure that helps alleviate the overfitting issue. We evaluate the quality of the refined generation by PAPO and other contenders on several benchmark datasets and a real-world molecule optimization task. Experimental results demonstrate the effectiveness of PAPO in producing high-quality refined generation without human supervision.

2. Related Work

Test-Time Alignment. Different from RLHF methods that directly update model parameters, recent studies have explored test-time alignment approaches that align LLMs with human preferences at inference time. *Best-of-N* (BoN) sampling (Lightman et al., 2024) selects the most preferred output from multiple candidates generated by the LLM using a reward model. To improve its efficiency, Speculative BoN accelerates generation by discarding low-quality responses early in the decoding process (Zhang et al., 2024). Building on BoN, TreeBoN further enhances inference-time alignment by a speculative tree-search framework (Qiu et al., 2024). TPO (Li et al., 2025) introduces an iterative refinement approach in which the model receives and incorporates textual feedback at test time to align its generations with implicit preferences.

Some prior works also explore prompt optimization for test-time alignment. For example, BPO first collects human feedback data, and then trains a prompt optimization model to guide the LLM toward generating more preferred responses (Cheng et al., 2024). However, this method still relies on human feedback for alignment. URIAL employs three fixed stylistic examples with a system prompt, achieving results comparable to RLHF (Lin et al., 2024). In contrast, our method jointly optimizes the prompt and downstream pseudo-supervision to achieve more tailored performance on specific tasks.

Self-Refinement. Self-refinement algorithms allow an LLM to generate initial responses on a downstream task, provide feedback on them, and iteratively refine its responses, leading to improved performance. For instance, LMSI employs CoT prompting (Wei et al., 2022) to generate high-quality labels for unlabeled datasets, which were then used to optimize the model (Huang et al., 2023). LLMRefine employs a fine-grained feedback model to identify defects in outputs and guide iterative refinements, optimizing performance during inference without additional training (Xu et al., 2024). Similarly, SALMON retrieves high-quality samples relevant to the downstream task and used them as ICL demonstrations to generate additional samples, which were then iteratively employed to fine-tune the LLM (Sun et al., 2024). ISARA is an improved self-refinement methods without human-crafted instructions and labeled rewards (Guo et al., 2024).

Several recent seminal works explored using ICL prompting for self-refinement without retraining model parameters (Wan et al., 2023a,b; Li et al., 2024). These methods first identify “high-confidence” pseudo-supervised data using carefully designed scoring functions, and then leverage the selected data as in-context demonstrations to guide final predictions. We further explore the pseudo-supervision across the entire downstream task as an implicit form of regularization to mitigate overfitting, drawing on well-established principles from self-supervised learning (Chapelle et al., 2006; Belkin et al., 2006).

Prompt Optimization. Prompt learning provides a lightweight alternative for enhancing the generation quality of LLMs on downstream tasks without requiring fine-tuning on model parameters. BBT optimizes the prompt for adaptation using derivative-free optimization techniques such as evolutionary algorithms (Sun et al., 2022). BDPL employs policy gradient algorithms to optimize the prompt (Diao et al., 2022). Typically, these methods still require labeled data to optimize the prompt.

3. Our Approach

In this section, we begin by introducing the notations, then describe the PAPO algorithm in detail, and finally provide a theoretical analysis of its properties in a simplified setting of classification.

3.1 Notations

In this part, we introduce the notations. Let $\mathbf{x}_l \in \mathcal{X}$ be the l -th query in the unsupervised dataset of size n , where \mathcal{X} is the textual space. We denote by $\mathbf{z} \in \mathcal{X}$ the prompt and \mathbf{z}_0 be the system default prompt. We define two functions associated with the LLM. First, let $\text{LLM}_{\text{opt}}(\cdot) : \mathbf{x} \mapsto \mathbf{p}$ denote the prompt optimization function, where $\mathbf{p} \in \mathcal{X}$. It takes a textual prompt (e.g., loss or gradient information) as input and outputs a response \mathbf{p} . To model the ICL capability of LLMs, we define the generation function as $\text{LLM}_{\text{gen}}(\cdot, \cdot, \cdot) : (\mathbf{x}, \mathbf{z}, D) \mapsto \mathbf{y}$, where \mathbf{x} is the query, $\mathbf{y} \in \mathcal{X}$ is the response in textual space, \mathbf{z} is the prompt, and $D = \{(\mathbf{x}_k, \hat{y}_k)\}_{k=1}^K$ is a set of K pseudo-supervised demonstrations drawn from the downstream task. D can be an empty set, e.g., $\text{LLM}_{\text{gen}}(\cdot, \mathbf{z}_0, \emptyset)$, indicating that the LLM is used with default prompt for prediction without demonstrations.

Following the formulation in TextGrad (Yuksekgonul et al., 2024), we use a prompting function $P_{\text{loss}}(\cdot | \cdot, \cdot, \cdot) : (\mathbf{z} | \mathbf{x}, \mathbf{y}, \mathbf{y}) \mapsto \mathbf{p}$ to represent the loss function (e.g., prediction consistency), where $\mathbf{p} \in \mathcal{X}$ denotes the loss expressed in textual format. The LLM then generates critiques that evaluate how well the pseudo-supervision \hat{y} , produced using prompt \mathbf{z} , addresses the query \mathbf{x} with its underlying supervision y . Formally, the loss $L(\mathbf{z})$ associated with prompt \mathbf{z} is defined as follows:

$$L(\mathbf{z}) := \text{LLM}_{\text{opt}}(P_{\text{loss}}(\mathbf{z} | \mathbf{x}, \hat{y}, y)) \quad (1)$$

Next, we define the prompting function $P_{\text{grad}}(\cdot)$, which incorporates the textual loss $L(\mathbf{z})$ to elicit update instructions, resulting in a textual gradient as follows:

$$\frac{\partial L}{\partial \mathbf{z}} := \text{LLM}_{\text{opt}}(P_{\text{grad}}(L(\mathbf{z}))) \quad (2)$$

Finally, we define the prompting function $P_{\text{update}}(\cdot)$, which applies the textual gradient to generate a refined variable, analogous to a gradient descent update, as follows:

$$\mathbf{z}_{\text{new}} = \text{LLM}_{\text{opt}}(P_{\text{update}}(\frac{\partial L}{\partial \mathbf{z}})) \quad (3)$$

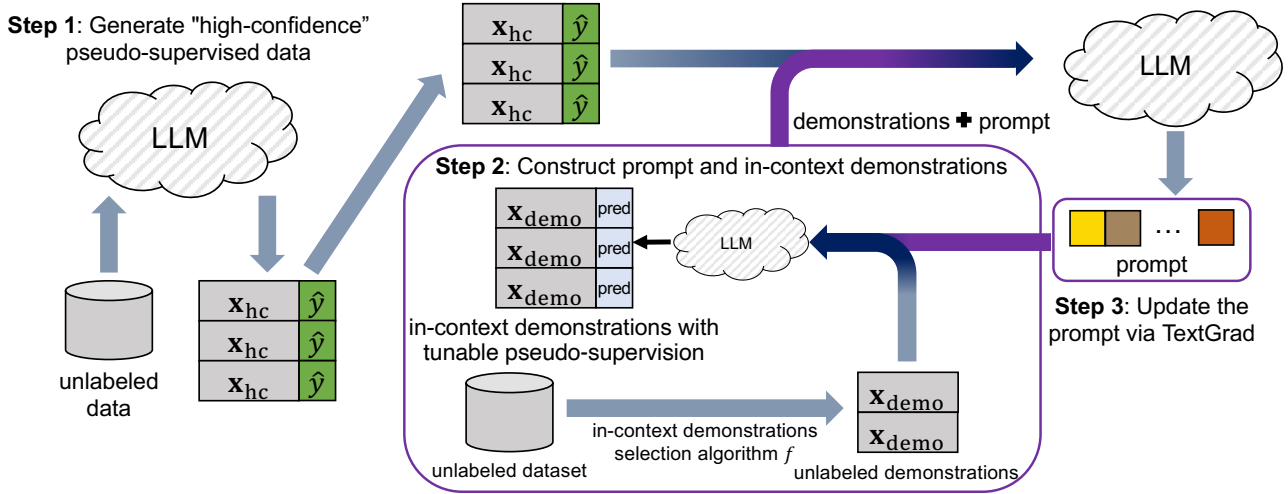
Since the downstream task is unsupervised, we propose to identify “high-confidence” pseudo-supervised data to optimize the prompt. Following the approach used in previous self-refinement methods (Huang et al., 2023), we adopt the self-consistency CoT (Wang et al., 2022) to identify “high-confidence” data and estimate the confidence of pseudo-supervised outputs with prompt \mathbf{z} . Specifically, we perform multiple-path decoding with a sampling temperature $T > 0$, automatically generating m reasoning paths with \mathbf{z} and corresponding answers $\{y_{l_1}, \dots, y_{l_m}\}$ for each query \mathbf{x}_l . We then apply majority voting (self-consistency) to select the most consistent and highest-confidence answer as \hat{y}_l , and define the confidence as follows (Huang et al., 2023):

$$c_l = \frac{1}{m} \sum_{j=1}^m \mathbb{1}(y_{l_j} = \hat{y}_l). \quad (4)$$

3.2 Pseudo-supervised Demonstrations Aligned Prompt Optimization

In this part, we present the proposed PAPO algorithm, which jointly optimizes the prompt and refines the pseudo-supervision for the downstream task in an iterative manner.

To optimize the prompt for specific downstream tasks, a straightforward approach is to generate the responses, identify “high-confidence” pseudo-supervised data, and then optimize the prompt based on



We iteratively identify “high-confidence” pseudo-supervised data and construct demonstrations for each data by selecting a set of data from the downstream task using a specific sample selection algorithm. Each selected sample is assigned pseudo-supervision generated by the LLM, guided by the current prompt and its corresponding demonstrations. We jointly refine the pseudo-supervision and optimize the prompt by learning with the “high-confidence” data, ensuring that the LLM’s predictions, generated based on the prompt and corresponding demonstrations, align with the original pseudo-supervision of the “high-confidence” data.

Figure 2: An illustration of the PAPO algorithm.

these data, following the principle idea from (Wan et al., 2023b; Guo et al., 2024; Li et al., 2024). For example, we optimize the following:

$$\arg \min_{\mathbf{z} \in \mathcal{Z}} \sum_{l=1}^n \mathbb{1}[c_l \geq \gamma] \cdot \text{LLM}_{\text{opt}}(P_{\text{loss}}(\mathbf{z} | \mathbf{x}_l, \text{LLM}_{\text{gen}}(\mathbf{x}_l, \mathbf{z}, \emptyset), \text{LLM}_{\text{gen}}(\mathbf{x}_l, \mathbf{z}_0, \emptyset))), \quad (5)$$

where $\mathbb{1}[\cdot]$ is the indicator function and $\gamma \in [0, 1]$ is a threshold for selecting “high-confidence” pseudo-supervised data in the downstream task.

Although learning prompts with “high-confidence” pseudo-supervised data is feasible, relying solely on such data may lead to overfitting, since the prompt training procedure in Eqn. (5) does not consider the use of the entire downstream dataset. To handle this problem, we propose to refine the pseudo-supervision for the entire unsupervised downstream task and optimize the prompt simultaneously. Since the in-context learning capability allows LLMs to implicitly learn a classifier from pseudo-supervised demonstrations and apply it to other data in downstream tasks, we define the objective function for prompt optimization with pseudo-supervised demonstrations as follows:

$$L_m(\mathbf{z}) = \sum_{l=1}^n \mathbb{1}[c_l \geq \gamma] \cdot \text{LLM}_{\text{opt}}(P_{\text{loss}}(\mathbf{z} | \mathbf{x}_l, \text{LLM}_{\text{gen}}(\mathbf{x}_l, \mathbf{z}, D_l), \text{LLM}_{\text{gen}}(\mathbf{x}_l, \mathbf{z}_0, \emptyset))), \quad (6)$$

where D_l is a set of in-context demonstrations for the query \mathbf{x}_l selected by algorithm $f(\mathbf{x}_l; \mathbf{z})$, with the pseudo-supervision of these demonstrations determined with the prompt \mathbf{z} . Specifically, $f(\mathbf{x}_l, \mathbf{z})$ outputs a set of pseudo-supervised demonstrations selected from the downstream task:

$$D_l = \{(\mathbf{x}_k, \text{LLM}_{\text{gen}}(\mathbf{x}_k, \mathbf{z}, \mathcal{D}_k)) | \mathbf{x}_k \in S_l\}_{k=1}^K,$$

where $\text{LLM}_{\text{gen}}(\mathbf{x}_k, \mathbf{z}, \mathcal{D}_k)$ is the pseudo-supervision of \mathbf{x}_k , guided by both \mathbf{z} and \mathcal{D}_k .

For demonstration selection, following the seminal works on in-context example selection (Liu et al., 2022; Min et al., 2022), we choose the K nearest samples for each input \mathbf{x}_l as its in-context demonstration set, denoted by S_l :

$$S_l = \arg \min_{\{k_j\}_{j=1}^K \subset \{1, \dots, n\}} \sum_{j=1}^K d(\mathbf{x}_l, \mathbf{x}_{k_j}), \quad (7)$$

where $d(\cdot, \cdot)$ is a distance measure between two queries. We follow the same procedure outlined in (Liu et al., 2022), introducing a sentence encoder $\theta(\cdot)$ and defining the distance as $d(\mathbf{x}_l, \mathbf{x}_k) = \|\theta(\mathbf{x}_l) - \theta(\mathbf{x}_k)\|_2$. In addition, to address majority label bias in the in-context demonstrations, we incorporate the plug-in de-biasing method (Zhao et al., 2021) into our algorithm in practice.

We illustrate the proposed PAPO algorithm in Figure 2 and summarize it with pseudo-code in Algorithm 1. We explore the entire downstream dataset by iteratively identifying "high-confidence" pseudo-supervised data, then simultaneously optimizing the prompt and refining the pseudo-supervision.

3.3 Theoretical Analysis

In this part, we provide theoretical insights to help explain why PAPO is effective. We emphasize that the presented theorem is standard and only serves to support our approach from a theoretical perspective; however, it is not intended as a theoretical contribution of this work.

The following theoretical analysis shows that PAPO refines generation in a way that encourages the pseudo-supervision to exhibit a clustering structure in the output space. In the simplified case of multi-class classification, PAPO encourages the refined labels to exhibit a multi-manifold structure, where each class occupies a disjoint convex region. When queries convey similar meanings, the refinement process encourages their labels to belong to the same class.

Recent seminal works have shown that ICL can be interpreted as a form of implicit empirical risk minimization (Min et al., 2022; Xie et al., 2022; Bai et al., 2023). We first introduce the following lemma in (Bai et al., 2023).

Lemma 1 (Corollary G.1 in (Bai et al., 2023)). *For any transformer with layer $L \geq 1$, under the same setting as Theorem G.1 in (Bai et al., 2023), the $(2L)$ -layer transformer TF_θ there approximates the true gradient descent trajectory $\{\mathbf{w}_{\text{GD}}^\ell\}_{\ell \geq 0}$: For the intermediate iterates $\{\hat{\mathbf{w}}^\ell\}_{\ell \in [L]}$ considered therein, we have*

$$\|\hat{\mathbf{w}}^\ell - \mathbf{w}_{\text{GD}}^\ell\|_2 \leq L_f^{-1} (1 + \eta L_f)^\ell \varepsilon,$$

where $L_f = \sup_{\mathbf{w} \in \mathcal{W}} \|\nabla^2 \hat{L}_N(\mathbf{w})\|_{\text{op}}$ denotes the smoothness of \hat{L}_N within \mathcal{W} .

Lemma 1 shows that transformers implement gradient descent on two-layer neural networks in-context. Similarly, the outputs of PAPO exhibit comparable behavior: for any pseudo-supervised example, when other pseudo-supervised examples are provided as in-context demonstrations, the model generates the same pseudo-label as when using the prompt. We build on this observation and Lemma 1 to make the following assumption about the refined outputs produced by PAPO.

Assumption 1 (Linear Separability). Consider a multi-class classification task, such as multiple-choice question answering. Let $\{x_1, \dots, x_n\} \subset \mathbb{R}^d$ be data points, and $y_i \in \{1, 2, \dots, K\}$ be multi-class labels refined by PAPO. Suppose there exists a linear multi-class classifier defined by K weight vectors $\{w_1, \dots, w_K\}$ and bias terms $\{b_1, \dots, b_K\}$ such that:

$$A(x) = \arg \max_{k=1, \dots, K} (w_k^\top x + b_k)$$

and for every i , $A(x_i) = y_i$.

We now show that linearly separable labels reveal an underlying clustering structure in the data.

Algorithm 1 Pseudo-supervised-demonstrations Aligned Prompt Optimization (PAPO)

- 1: Set total number of iterations T , number of in-context demonstrations K , total number of sampling m for confidence estimation, and confidence threshold γ .
- 2: **for** $t = 1$ **to** T **do**
- 3: **Stochastic sampling:** Sample a mini-batch of data from the downstream task
- 4: **Confidence estimation:** Estimate the confidence by Eqn. (4) with $\mathbf{z}^{(t)}$
- 5: **Compute loss:** Compute loss by Eqn. (6) and generate gradient by Eqn. (2)
- 6: **Update prompt:** $\mathbf{z}^{(t+1)} = \text{LLM}_{\text{opt}}(P_{\text{update}}(\frac{\partial L}{\partial \mathbf{z}^{(t)}}))$
- 7: **Refine output:** $\forall l \in [n], \hat{y}_l = \text{LLM}_{\text{gen}}(\mathbf{x}_l, \mathbf{z}^{(t+1)}, D_l)$
- 8: **end for**

Theorem 1. Suppose the linear separability in Assumption 1 holds. For each class k , the class-specific sample set $S_k := \{x_i \mid y_i = k\}$ is contained in a convex polyhedral region

$$R_k := \left\{ x \in \mathbb{R}^d \mid w_k^\top x + b_k > w_j^\top x + b_j, \forall j \neq k \right\},$$

with pairwise disjointness

$$R_k \cap R_j = \emptyset, \quad \forall k \neq j,$$

and separation

$$\text{dist}(R_k, R_j) > 0.$$

Theorem 1 shows that the geometry of the pseudo-supervision refined by PAPO exhibits a low-dimensional, cluster-aligned structure that aligns with the clustering induced by graph Laplacian minimization. Detailed proofs are deferred to the Appendix B.

4. Experiments

In this section, we evaluate the proposed PAPO algorithm alongside several contenders using a range of benchmarks. We then conduct ablation studies to assess the contribution of each component in our approach. Finally, we apply the proposed method to a real world molecular optimization task.

4.1 Experimental Setup

Tasks and Datasets. We evaluate PAPO on three tasks: two benchmarks (question answering and natural language inference) and one real-world application (molecule optimization).

Question Answering. We use google-proof question answering (GPQA) dataset (Rein et al., 2024), SimpleQA dataset (Wei et al., 2024), and the MMLU subsets (Hendrycks et al., 2021) astronomy (AST), high-school-cs (HSCS), high-school-mathematics (HSM), college-mathematics (Cmath), college-cs (CCS), college-medicine (CMed), management (MAN), marketing (MAR), and all-random (RND).

Natural Language Inference. We use the GLUE subsets (Wang et al., 2018), CoLA, SST-2, QQP, MRPC, MNLI, WNLI, and RTE, which contain sentences labeled as entailment, neutrality, or contradiction.

Molecule Optimization: We also evaluate PAPO on a real-world molecular optimization task using the DOCKSTRING dataset (García-Ortegón et al., 2022). Each molecule is represented as a SMILES string (Yuksekgonul et al., 2024), and the learning problem is to generate an improved version that surpasses the original in terms of important chemical properties, specifically the Vina score, which reflects binding affinity, and the QED score, which measures drug-likeness (Trott and Olson, 2010).

Table 1: Performance comparisons across **Question Answering** (QA), **Natural Language Inference** (NLI) tasks. We report the average accuracy (%) and standard deviation over 5 runs. The best results are in **bold** and $(\uparrow \cdot)$ indicates the improvement over Direct in terms of average accuracy.

Task	Dataset	Direct	ICL	Auto-CoT	USP	SR (BDPL)	SR (RLprompt)	PAPO
QA	GPQA	37.9 \pm 1.3	37.3 \pm 0.9	38.4 \pm 0.5	38.6 \pm 0.7	37.9 \pm 1.0	37.5 \pm 0.9	39.9 \pm 0.6 $(\uparrow 2.0)$
	SimpleQA	38.2 \pm 0.8	37.5 \pm 1.2	38.9 \pm 1.0	38.2 \pm 0.9	38.1 \pm 1.3	37.4 \pm 1.1	39.6 \pm 0.9 $(\uparrow 1.4)$
	MAR	90.2 \pm 2.0	90.7 \pm 1.7	88.9 \pm 1.7	92.4 \pm 0.9	91.3 \pm 1.8	91.0 \pm 0.8	92.1 \pm 0.8 $(\uparrow 1.9)$
	MAN	76.8 \pm 1.4	76.4 \pm 1.0	76.5 \pm 1.0	77.5 \pm 1.6	79.0 \pm 1.2	78.2 \pm 0.9	81.1 \pm 1.4 $(\uparrow 4.3)$
	HSM	50.9 \pm 2.9	47.5 \pm 2.2	47.4 \pm 2.2	51.4 \pm 2.3	53.4 \pm 1.8	53.2 \pm 1.1	55.6 \pm 1.6 $(\uparrow 4.7)$
	HCS	90.8 \pm 2.7	91.0 \pm 2.1	89.1 \pm 2.1	89.9 \pm 2.3	92.5 \pm 2.1	91.3 \pm 2.2	93.1 \pm 1.4 $(\uparrow 2.3)$
	CMed	61.9 \pm 1.8	58.4 \pm 3.4	58.4 \pm 3.4	61.8 \pm 2.1	61.4 \pm 1.7	59.5 \pm 3.0	63.8 \pm 2.3 $(\uparrow 1.9)$
	CMath	40.7 \pm 4.2	40.8 \pm 2.5	40.2 \pm 2.5	41.1 \pm 2.8	44.3 \pm 2.7	43.3 \pm 1.3	46.1 \pm 1.6 $(\uparrow 5.4)$
	CCS	68.4 \pm 2.4	71.5 \pm 1.3	69.6 \pm 1.3	69.8 \pm 2.3	71.8 \pm 1.8	71.0 \pm 1.6	73.2 \pm 1.0 $(\uparrow 4.8)$
	AST	86.6 \pm 2.5	86.8 \pm 2.3	86.5 \pm 2.3	87.1 \pm 2.1	85.6 \pm 3.6	88.0 \pm 2.8	87.2 \pm 1.5 $(\uparrow 0.6)$
	RND	68.7 \pm 1.1	68.9 \pm 1.2	68.3 \pm 1.2	70.4 \pm 1.7	70.6 \pm 1.7	70.5 \pm 1.3	72.8 \pm 2.0 $(\uparrow 4.1)$
NLI	MNLI	91.7 \pm 2.3	90.4 \pm 2.0	90.4 \pm 2.0	90.8 \pm 1.1	92.8 \pm 1.6	92.1 \pm 0.8	92.0 \pm 1.8 $(\uparrow 0.3)$
	QQP	71.5 \pm 1.0	71.6 \pm 2.0	68.6 \pm 2.0	71.8 \pm 1.6	71.9 \pm 1.6	69.3 \pm 3.1	73.2 \pm 2.0 $(\uparrow 1.7)$
	SST-2	89.6 \pm 1.5	88.4 \pm 0.7	88.4 \pm 0.7	90.0 \pm 1.9	90.3 \pm 2.1	89.6 \pm 2.0	92.7 \pm 1.1 $(\uparrow 3.1)$
	MRPC	90.9 \pm 2.0	91.0 \pm 1.5	90.1 \pm 1.5	69.8 \pm 2.8	90.9 \pm 1.0	90.1 \pm 1.8	93.4 \pm 1.7 $(\uparrow 2.5)$
	CoLA	69.7 \pm 1.7	69.7 \pm 2.3	65.8 \pm 2.3	68.9 \pm 2.3	67.4 \pm 2.9	69.9 \pm 1.3	71.2 \pm 1.1 $(\uparrow 1.5)$
	WNLI	90.8 \pm 1.6	87.3 \pm 1.7	87.3 \pm 1.7	89.0 \pm 2.3	88.8 \pm 2.0	88.5 \pm 1.8	91.1 \pm 1.4 $(\uparrow 1.1)$
	RTE	92.9 \pm 1.2	93.1 \pm 1.0	88.7 \pm 1.0	70.5 \pm 2.1	91.9 \pm 1.3	90.0 \pm 1.5	94.9 \pm 1.6 $(\uparrow 2.0)$

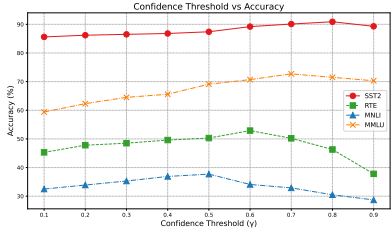
Contenders. We compare our proposed algorithm against one baseline and five strong contenders. The baseline is **Direct**, where the LLM is prompted with the default prompt to generate predictions. We include **Auto-CoT** (Zhang et al., 2022) as a contender, which automatically generates intermediate reasoning steps in inference. This encourages the LLM to follow a CoT process before producing a final answer, improving generation quality on downstream tasks. Moreover, we include **USP** (Wan et al., 2023b), which uses carefully designed scoring functions to select “high-confidence” data and applies ICL for prediction.

For the other three contenders, we identify the “high-confidence” pseudo-supervised examples using the same mechanism as in the proposed PAPO algorithm. Based on these examples, we apply **ICL** (Liu et al., 2022), using these examples as demonstrations to predict the remaining unlabeled instances. We further include two approaches that integrate prompt learning algorithms with the self-refinement strategy proposed by Huang et al. (2023): **SR (BDPL)** (Diao et al., 2022) and **SR (RLprompt)** (Deng et al., 2022). Specifically, SR (BDPL) employs a policy gradient method to optimize prompts based on the “high-confidence” pseudo-labeled data, while SR (RLprompt) uses a parameter-efficient policy network that adaptively generates prompts conditioned on these “high-confidence” pseudo-labeled examples. For both the SR (BDPL) and SR (RLprompt) algorithms, we use the default parameter settings from their original papers. Moreover, we incorporated the plug-in de-bias method (Zhao et al., 2021) in all contenders.

Implementation Details. In all experiments, we used GPT-4o¹ and GPT-4o-mini², provided by OpenAI, where GPT-4o-mini is much cheaper than GPT-4o. In all experiments, except for the ablation study on the choice of LLM, we use GPT-4o. Due to page limits, more implementation details on hyperparameters setting and prompts design are provided in Appendix C.

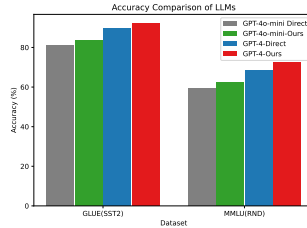
In some real-world tasks, users may prefer a customized model instead of relying on refined generation for downstream applications. To support this, we use the refined pseudo-supervision and apply OpenAI’s commercial fine-tuning service to obtain a customized model. Fine-tuning is performed using the official OpenAI API³.

1. <https://platform.openai.com/docs/models/gpt-4o>
 2. <https://platform.openai.com/docs/models/gpt-4o-mini>
 3. <https://platform.openai.com/docs/guides/fine-tuning>

(a) Acc. on different γ .

Method	SST-2	GPQA	SimpleQA
Direct	89.6/5.5	37.9/5.9	38.2/5.8
USP	90.0/9.6	38.6/10.1	38.2/9.8
ICL	88.4/10.4	37.3/10.7	37.5/10.5
SR (BDPL)	90.3/11.3	37.9/10.8	38.1/11.6
PAPO	92.7/13.5	39.9/13.9	39.9/14.1

(b) Acc. (%) and Runtime (s).



(c) Acc. on different LLMs.

Figure 3: Ablation studies of the PAPO algorithm.

4.2 Performance Comparison on Benchmarks

In this section, we compare the proposed PAPO algorithm with other contenders on benchmark datasets. We set all termination $T = 10$. For both ICL and PAPO, the number of demonstrations is set to 5. The confidence threshold is fixed at $\gamma = 0.65$ for PAPO and all competing methods.

We first report the average accuracy and standard deviation of the refined generations by the proposed PAPO algorithm and other contenders on question answering and natural language inference tasks, as shown in Table 1. The proposed PAPO algorithm consistently outperforms nearly all other methods across the evaluated datasets. Compared to the Direct algorithm and the Auto-CoT method, our approach achieves superior performance, demonstrating the effectiveness of leveraging downstream unsupervised data and prompt optimization to refine model generation. Furthermore, the proposed PAPO algorithm outperforms USP, SR (BDPL), and SR (RLPrompt), highlighting the importance of refining in-context pseudo-supervised demonstrations during the learning process, rather than solely relying on “high-confidence” data to predict the remaining examples.

In certain cases, users may prefer a customized model over refined generation for downstream tasks. To evaluate the performance of the fine-tuned model for both the proposed method and the baselines, we first learn the prompt and pseudo-supervision using 20% of the original dataset. The model is then fine-tuned on this refined dataset and evaluated on the remaining 80% of the data. Our proposed method consistently outperforms other contenders, indicating higher quality in the refined generation compared to existing approaches. Due to space constraints, additional comparison results for customized models fine-tuned with the refined outputs from all contenders and PAPO are provided in Appendix A, example outputs on the benchmark datasets are provided in Appendix D.

4.3 Ablation Studies

In this part, we conduct ablation studies on the proposed PAPO algorithm, analyzing the impact of generation of “high-confidence” pseudo-supervised data, the selection of in-context demonstrations, the computational overhead of PAPO, and the choice of LLM used in the pipeline.

Generation of “high-confidence” pseudo-supervised data. We first investigate the confidence threshold γ for generating “high-confidence” pseudo-labeled data. Experiments are conducted across both the question answering and natural language inference tasks, using average accuracy as the evaluation metric. The results are presented in Figure 3(a). We observe that setting the confidence threshold between 0.6 and 0.7 yields stable and satisfactory performance across all experiments. A lower threshold may introduce incorrect pseudo-labels, negatively affecting performance, while a higher threshold can limit the amount of selected pseudo-supervised data, also leading to performance degradation. Based on these findings, we recommend setting the confidence threshold in the range of 0.6 to 0.7 for practical applications.

Computational overhead of PAPO. Next, we analyze the computational overhead of PAPO. Our method incurs additional overhead from computing the distance matrix for the unlabeled data and performing pseudo-supervision refinement during each round of prompt updating. We empirically compare

Table 2: Performance comparisons with varying number of in-context demonstrations on benchmark datasets. We report the average accuracy (%) and standard deviation over 5 runs. The best results are in **bold**.

Method	MNLI	QQP	SST-2	MRPC	CoLA	WNLI	RTE	RND
Direct	91.7 ± 2.3	71.4 ± 1.0	89.6 ± 1.5	90.9 ± 2.0	69.7 ± 1.7	90.8 ± 1.6	92.9 ± 1.2	68.7 ± 1.1
ICL ($k = 3$)	89.3 ± 1.9	68.5 ± 2.1	88.9 ± 2.4	88.3 ± 1.7	66.4 ± 2.3	87.5 ± 1.7	88.3 ± 1.2	67.5 ± 1.5
ICL ($k = 5$)	90.4 ± 2.0	71.6 ± 2.0	88.4 ± 0.7	91.0 ± 1.5	69.7 ± 2.3	87.3 ± 1.7	93.1 ± 1.0	68.9 ± 1.2
PAPO ($k = 3$)	91.5 ± 2.1	72.5 ± 2.1	91.3 ± 1.7	92.3 ± 1.8	71.8 ± 1.5	91.0 ± 1.7	93.1 ± 2.0	71.5 ± 2.6
PAPO ($k = 5$)	92.0 ± 1.8	73.2 ± 2.0	92.7 ± 1.1	93.4 ± 1.7	71.2 ± 1.1	91.1 ± 1.4	94.9 ± 1.6	72.8 ± 2.0

the average accuracy and average runtime (10 rounds) of our method against other methods, as reported in Figure 3(b). The results show PAPO achieves better performance with an acceptable increase in computational and time resources.

Choice of LLM used in the pipeline. We then evaluate the performance of the PAPO algorithm with different LLMs. Experiments are conducted on both question answering and natural language inference tasks, with the number of demonstrations fixed at 5 for fair comparison. Figure 3(c) presents the average accuracy on unlabeled data using GPT-4o and GPT-4o-mini. The proposed algorithm achieves higher accuracy with GPT-4o than with GPT-4o-mini, which aligns with the relative capabilities of the two models. These results suggest that PAPO benefits from stronger LLMs, leading to improved performance.

Selection of in-context demonstrations. Finally, we investigate the impact of the number of in-context demonstrations by selecting different numbers of K -nearest samples for each query, following the distance metric used in (Liu et al., 2022). The comparison results are reported in Table 2. It can be observed that the PAPO algorithm outperforms both the Direct and ICL methods on nearly all datasets across different values of K . This highlights the benefit of leveraging pseudo-supervised data as in-context demonstrations during the prompt optimization phase. Based on our empirical results, setting $K = 5$ is recommended to achieve satisfactory performance.

4.4 Molecule Optimization

In this part, we apply the proposed PAPO algorithm to a real world drug molecular optimization task. The supervision for each molecule is defined by the optimal counterparts, evaluated based on the Vina score and QED score. We begin with five clinically approved drugs from the dataset as the initial set of “high-confidence” pseudo-supervised data. GPT-4o is used as the LLM, with the prompt text adopted from TextGrad (Yuksekgonul et al., 2024).

In Figure 4, we present the drug molecules refined by the proposed PAPO in the final three iterations, alongside the molecule refined by Auto-CoT and three clinically approved drugs Ciprofibrate, Fenofibrate, and Fenofibric acid. We observe that the molecule refined by PAPO is structurally close to clinically approved drugs, while achieving better QED and Vina scores and outperforming the Auto-CoT method.

Based on this empirical result, PAPO explores the entire unsupervised dataset to generate more refined outputs,

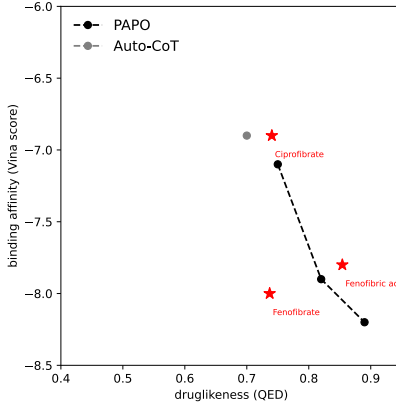


Figure 4: Vina score and QED score of the molecules refined by PAPO and Auto-CoT compared to clinically approved compounds. The molecule refined by PAPO exhibits greater structural similarity to its closest approved counterpart while achieving better QED and Vina scores.

while leveraging the TextGrad framework to produce explainable decisions, which allow researchers to clearly understand how and why a molecule’s structure is generated. These results underscore the promising potential of the proposed PAPO algorithm in scientific discovery tasks.

5. Conclusion

In this paper, we investigate test-time pseudo-supervision refinement without retraining model parameters or relying on human supervision. A direct solution is to use “high-confidence” pseudo-supervised data for in-context prompting or prompt tuning, but relying solely on such data can lead to the overfitting issue. We propose PAPO, a novel algorithm that iteratively identifies “high-confidence” pseudo-supervised data and jointly optimizes the prompt and refines the pseudo-supervision. We regularize the refined pseudo-supervised data to exhibit internal consistency: when used as in-context demonstrations, they guide the LLM to generate consistent outputs on the “high-confidence” pseudo-supervised data. Theoretical analysis shows that, in a simplified multi-class classification setting, PAPO encourages pseudo-supervision to form a low-dimensional structure aligned with graph Laplacian clustering, helping to mitigate overfitting and improve generalization. Experiments on question answering and natural language inference benchmarks, and a real-world molecule optimization task, show the effectiveness of PAPO. The refined pseudo-supervised data can further be used to obtain a customized model with commercial fine-tuning service, and the experimental results also show the superiority of the proposed PAPO algorithm.

References

J. Achiam, S. Adler, S. Agarwal, L. Ahmad, I. Akkaya, F. L. Aleman, D. Almeida, J. Altenschmidt, S. Altman, S. Anadkat, et al. Gpt-4 technical report. *arXiv preprint arXiv:2303.08774*, 2023.

Y. Bai, F. Chen, H. Wang, C. Xiong, and S. Mei. Transformers as statisticians: Provable in-context learning with in-context algorithm selection. *Advances in Neural Information Processing Systems (NeurIPS)*, 36:57125–57211, 2023.

M. Belkin, P. Niyogi, and V. Sindhwani. Manifold regularization: A geometric framework for learning from labeled and unlabeled examples. *Journal of Machine Learning Research*, 7(11), 2006.

C. M. Bishop. *Pattern Recognition and Machine Learning*. Springer, 2006.

T. Brown, B. Mann, N. Ryder, M. Subbiah, J. D. Kaplan, P. Dhariwal, A. Neelakantan, P. Shyam, G. Sastry, A. Askell, et al. Language models are few-shot learners. *Advances in Neural Information Processing Systems (NeurIPS)*, 33:1877–1901, 2020.

O. Chapelle, B. Schölkopf, and A. Zien. *Semi-Supervised Learning*. MIT Press, 2006.

J. Cheng, X. Liu, K. Zheng, P. Ke, H. Wang, Y. Dong, J. Tang, and M. Huang. Black-box prompt optimization: Aligning large language models without model training. In *Proceedings of the 62nd Annual Meeting of the Association for Computational Linguistics (ACL)*, pages 3201–3219, 2024.

M. Deng, J. Wang, C.-P. Hsieh, Y. Wang, H. Guo, T. Shu, M. Song, E. Xing, and Z. Hu. Rlprompt: Optimizing discrete text prompts with reinforcement learning. In *Proceedings of the 2022 Conference on Empirical Methods in Natural Language Processing (EMNLP)*, pages 3369–3391, 2022.

S. Diao, Z. Huang, R. Xu, X. Li, L. Yong, X. Zhou, and T. Zhang. Black-box prompt learning for pre-trained language models. *Transactions on Machine Learning Research*, 2022.

M. García-Ortegón, G. N. Simm, A. J. Tripp, J. M. Hernández-Lobato, A. Bender, and S. Bacallado. Dockstring: easy molecular docking yields better benchmarks for ligand design. *Journal of Chemical Information and Modeling*, 62(15):3486–3502, 2022.

I. Goodfellow, Y. Bengio, and A. Courville. *Deep Learning*. MIT Press, 2016.

H. Guo, Y. Yao, W. Shen, J. Wei, X. Zhang, Z. Wang, and Y. Liu. Human-instruction-free llm self-alignment with limited samples. *arXiv preprint arXiv:2401.06785*, 2024.

D. Hendrycks, C. Burns, S. Basart, A. Zou, M. Mazeika, D. Song, and J. Steinhardt. Measuring massive multitask language understanding. In *The 10th International Conference on Learning Representations (ICLR)*, 2021.

J. Huang, S. S. Gu, L. Hou, Y. Wu, X. Wang, H. Yu, and J. Han. Large language models can self-improve. In *Proceedings of the 2023 Conference on Empirical Methods in Natural Language Processing (EMNLP)*, pages 1051–1068, 2023.

R. Li, G. Wang, and J. Li. Are human-generated demonstrations necessary for in-context learning? In *The 12th International Conference on Learning Representations*, 2024.

Y. Li, X. Hu, X. Qu, L. Li, and Y. Cheng. Test-time preference optimization: On-the-fly alignment via iterative textual feedback. *arXiv preprint arXiv:2501.12895*, 2025.

H. Lightman, V. Kosaraju, Y. Burda, H. Edwards, B. Baker, T. Lee, J. Leike, J. Schulman, I. Sutskever, and K. Cobbe. Let’s verify step by step. In *The 12th International Conference on Learning Representations*, 2024.

B. Y. Lin, A. Ravichander, X. Lu, N. Dziri, M. Sclar, K. Chandu, C. Bhagavatula, and Y. Choi. The unlocking spell on base llms: Rethinking alignment via in-context learning. In *The 12th International Conference on Learning Representations*, 2024.

J. Liu, D. Shen, Y. Zhang, W. B. Dolan, L. Carin, and W. Chen. What makes good in-context examples for gpt-3? In *The 3rd Workshop on Knowledge Extraction and Integration for Deep Learning Architectures*, pages 100–114, 2022.

S. Min, X. Lyu, A. Holtzman, M. Artetxe, M. Lewis, H. Hajishirzi, and L. Zettlemoyer. Rethinking the role of demonstrations: What makes in-context learning work? In *Proceedings of the 2022 Conference on Empirical Methods in Natural Language Processing (EMNLP)*, pages 11048–11064, 2022.

L. Ouyang, J. Wu, X. Jiang, D. Almeida, C. Wainwright, P. Mishkin, C. Zhang, S. Agarwal, K. Slama, A. Ray, et al. Training language models to follow instructions with human feedback. *Advances in Neural Information Processing Systems (NeurIPS)*, 35:27730–27744, 2022.

J. Qiu, Y. Lu, Y. Zeng, J. Guo, J. Geng, H. Wang, K. Huang, Y. Wu, and M. Wang. Treebon: Enhancing inference-time alignment with speculative tree-search and best-of-n sampling. *arXiv preprint arXiv:2410.16033*, 2024.

R. Rafailov, A. Sharma, E. Mitchell, C. D. Manning, S. Ermon, and C. Finn. Direct preference optimization: Your language model is secretly a reward model. *Advances in Neural Information Processing Systems (NeurIPS)*, 36:53728–53741, 2023.

D. Rein, B. L. Hou, A. C. Stickland, J. Petty, R. Y. Pang, J. Dirani, J. Michael, and S. R. Bowman. Gpqa: A graduate-level google-proof q&a benchmark. In *First Conference on Language Modeling*, 2024.

T. Sun, Y. Shao, H. Qian, X. Huang, and X. Qiu. Black-box tuning for language-model-as-a-service. In *Proceedings of the 39th International Conference on Machine Learning (ICML)*, pages 20841–20855, 2022.

Z. Sun, Y. Shen, Q. Zhou, H. Zhang, Z. Chen, D. Cox, Y. Yang, and C. Gan. Principle-driven self-alignment of language models from scratch with minimal human supervision. *Advances in Neural Information Processing Systems (NeurIPS)*, 36:2511–2565, 2024.

O. Trott and A. J. Olson. Autodock vina: improving the speed and accuracy of docking with a new scoring function, efficient optimization, and multithreading. *Journal of computational chemistry*, 31(2):455–461, 2010.

X. Wan, R. Sun, H. Dai, S. Arik, and T. Pfister. Better zero-shot reasoning with self-adaptive prompting. In *Findings of the 61st Annual Meeting of the Association for Computational Linguistics (ACL)*, pages 3493–3514, 2023a.

X. Wan, R. Sun, H. Nakhost, H. Dai, J. M. Eisenschlos, S. O. Arik, and T. Pfister. Universal self-adaptive prompting. In *The 2023 Conference on Empirical Methods in Natural Language Processing (EMNLP)*, pages 7437–7462, 2023b.

A. Wang, A. Singh, J. Michael, F. Hill, O. Levy, and S. Bowman. Glue: A multi-task benchmark and analysis platform for natural language understanding. In *Proceedings of the 2018 EMNLP Workshop BlackboxNLP: Analyzing and Interpreting Neural Networks for NLP*, pages 353–355, 2018.

X. Wang, J. Wei, D. Schuurmans, Q. V. Le, E. H. Chi, S. Narang, A. Chowdhery, and D. Zhou. Self-consistency improves chain of thought reasoning in language models. In *The 11th International Conference on Learning Representations (ICLR)*, 2022.

Y. Wang, Y. Kordi, S. Mishra, A. Liu, N. A. Smith, D. Khashabi, and H. Hajishirzi. Self-instruct: Aligning language models with self-generated instructions. In *Proceedings of the 61st Annual Meeting of the Association for Computational Linguistics (ACL)*, pages 13484–13508, 2023.

J. Wei, X. Wang, D. Schuurmans, M. Bosma, F. Xia, E. Chi, Q. V. Le, D. Zhou, et al. Chain-of-thought prompting elicits reasoning in large language models. *Advances in Neural Information Processing Systems (NeurIPS)*, 35:24824–24837, 2022.

J. Wei, N. Karina, H. W. Chung, Y. J. Jiao, S. Papay, A. Glaese, J. Schulman, and W. Fedus. Measuring short-form factuality in large language models. *arXiv preprint arXiv:2411.04368*, 2024.

S. M. Xie, A. Raghunathan, P. Liang, and T. Ma. An explanation of in-context learning as implicit bayesian inference. In *The 11th International Conference on Learning Representations*, 2022.

W. Xu, D. Deutsch, M. Finkelstein, J. Juraska, B. Zhang, Z. Liu, W. Y. Wang, L. Li, and M. Freitag. Llmrefine: Pinpointing and refining large language models via fine-grained actionable feedback. In *Findings of the Association for Computational Linguistics (NAACL)*, pages 1429–1445, 2024.

A. Yang, B. Yang, B. Zhang, B. Hui, B. Zheng, B. Yu, C. Li, D. Liu, F. Huang, H. Wei, et al. Qwen2. 5 technical report. *arXiv preprint arXiv:2412.15115*, 2024.

M. Yuksekgonul, F. Bianchi, J. Boen, S. Liu, Z. Huang, C. Guestrin, and J. Zou. Textgrad: Automatic” differentiation” via text. *arXiv preprint arXiv:2406.07496*, 2024.

R. Zhang, M. Haider, M. Yin, J. Qiu, M. Wang, P. Bartlett, and A. Zanette. Accelerating best-of-n via speculative rejection. In *ICML 2024 Workshop on Structured Probabilistic Inference and Generative Modeling*, 2024.

Z. Zhang, A. Zhang, M. Li, and A. Smola. Automatic chain of thought prompting in large language models. In *The 11th International Conference on Learning Representations (ICLR)*, 2022.

Z. Zhao, E. Wallace, S. Feng, D. Klein, and S. Singh. Calibrate before use: Improving few-shot performance of language models. In *Proceedings of the 38th International Conference on Machine Learning (ICML)*, pages 12697–12706, 2021.

Appendix

Appendix A. Additional Experimental Results

In this section, we report the performance of fine-tuned models on benchmark datasets. As shown in Table 3, we compare models fine-tuned on pseudo-supervised datasets generated by PAPO and other methods. Results show that the model trained with PAPO achieves better performance. Notably, consistent improvements in pseudo-supervised data quality directly translate to better fine-tuning results, highlighting the superiority of the proposed PAPO algorithm.

Table 3: Performance comparisons across **Question Answering** (QA), **Natural Language Inference** (NLI) tasks. We report the average accuracy (%) and standard deviation over 5 runs. The best results are in **bold**.

Task	Dataset	Direct	ICL	Auto-CoT	USP	SR (BDPL)	SR (RLprompt)	PAPO
QA	GPQA	38.5 ± 1.7	38.7 ± 1.0	39.5 ± 0.7	39.5 ± 0.2	38.2 ± 1.5	37.8 ± 1.2	40.1 ± 0.3 ($\uparrow 1.6$)
	SimpleQA	38.6 ± 0.4	37.9 ± 1.0	39.4 ± 0.9	39.0 ± 0.9	38.8 ± 1.6	37.9 ± 0.8	40.6 ± 0.9 ($\uparrow 2.0$)
	MAR	91.1 ± 2.3	88.9 ± 1.5	89.9 ± 1.3	92.7 ± 1.1	91.5 ± 1.7	92.4 ± 0.4	93.6 ± 0.8 ($\uparrow 2.5$)
	MAN	76.9 ± 1.1	77.8 ± 1.5	77.0 ± 1.3	78.5 ± 2.0	79.5 ± 1.6	79.0 ± 1.0	82.0 ± 1.8 ($\uparrow 5.1$)
	HSM	51.1 ± 2.8	47.9 ± 2.0	47.6 ± 2.2	52.0 ± 1.9	54.0 ± 2.1	53.7 ± 0.7	56.9 ± 2.1 ($\uparrow 5.8$)
	HCS	91.6 ± 2.5	89.6 ± 2.4	89.7 ± 1.8	91.6 ± 1.8	93.7 ± 2.0	92.2 ± 1.7	94.1 ± 1.7 ($\uparrow 2.5$)
	CMed	62.9 ± 1.5	59.9 ± 2.9	59.4 ± 3.0	62.6 ± 2.5	62.7 ± 1.9	61.2 ± 2.6	64.1 ± 2.4 ($\uparrow 1.2$)
	CMath	41.6 ± 4.0	41.2 ± 2.3	41.3 ± 2.0	42.4 ± 2.9	45.1 ± 2.6	44.3 ± 1.6	47.2 ± 1.8 ($\uparrow 5.6$)
	CCS	69.7 ± 2.0	70.8 ± 1.4	70.6 ± 1.1	70.6 ± 2.5	72.9 ± 1.6	72.4 ± 1.8	74.7 ± 1.3 ($\uparrow 5.0$)
	AST	87.4 ± 2.6	87.7 ± 2.4	87.3 ± 2.1	88.5 ± 2.1	86.7 ± 3.1	89.1 ± 2.4	88.7 ± 1.9 ($\uparrow 1.3$)
NLI	RND	69.4 ± 1.3	69.3 ± 1.4	69.5 ± 1.1	71.3 ± 1.4	71.9 ± 1.4	71.6 ± 1.0	73.8 ± 1.8 ($\uparrow 4.4$)
	MNLI	92.2 ± 2.1	91.2 ± 1.6	91.4 ± 1.8	91.6 ± 1.0	93.8 ± 1.6	92.7 ± 1.0	93.5 ± 1.4 ($\uparrow 1.3$)
	QQP	72.2 ± 0.9	69.6 ± 1.7	69.7 ± 1.5	73.1 ± 1.5	73.0 ± 1.8	70.7 ± 2.8	74.5 ± 2.1 ($\uparrow 2.3$)
	SST-2	90.8 ± 1.6	89.8 ± 0.8	89.7 ± 0.9	91.2 ± 1.8	91.4 ± 2.3	90.7 ± 2.1	93.8 ± 1.3 ($\uparrow 3.0$)
	MRPC	91.6 ± 2.1	90.8 ± 1.4	91.1 ± 1.7	70.9 ± 2.9	92.1 ± 1.2	91.2 ± 1.7	94.5 ± 1.6 ($\uparrow 2.9$)
	CoLA	70.7 ± 1.6	66.9 ± 2.1	66.9 ± 2.4	70.1 ± 2.5	68.7 ± 2.6	71.1 ± 1.1	72.2 ± 1.3 ($\uparrow 1.5$)
	WNLI	91.9 ± 1.4	88.7 ± 1.4	88.9 ± 1.8	90.0 ± 2.2	89.9 ± 2.0	89.6 ± 1.5	92.8 ± 1.7 ($\uparrow 0.9$)
	RTE	94.1 ± 1.3	89.5 ± 1.2	89.6 ± 1.1	72.0 ± 1.8	93.1 ± 1.1	91.4 ± 1.2	96.2 ± 1.7 ($\uparrow 2.1$)

Appendix B. Proof of Theorem 1

By the assumption that $A(x_i) = y_i$, we have for each i with $y_i = k$:

$$w_k^\top x_i + b_k > w_j^\top x_i + b_j, \quad \forall j \neq k.$$

Therefore, x_i lies in the region

$$R_k := \left\{ x \in \mathbb{R}^d \mid w_k^\top x + b_k > w_j^\top x + b_j \quad \forall j \neq k \right\},$$

which is the intersection of $K - 1$ open half-spaces and hence is a convex open polyhedron.

Because the regions are defined by strict inequalities, any two distinct regions R_k and R_j are disjoint:

$$R_k \cap R_j = \emptyset, \quad \forall k \neq j.$$

Furthermore, since each x_i lies in one of finitely many disjoint convex regions, and the dataset is finite, there exists a minimum separation margin:

$$\delta := \min_{\substack{x \in S_k, x' \in S_j \\ k \neq j}} \|x - x'\| > 0.$$

Assume now that the data points $\{x_i\}$ are sampled from a smooth probability distribution \mathbb{P} supported on a compact subset of \mathbb{R}^d . Then, for each class k , the conditional distribution $\mathbb{P}(x \mid y = k)$ is supported within R_k .

Since R_k is convex and bounded (from finite data), and \mathbb{P} is smooth, the support of $\mathbb{P}(x \mid y = k)$ is a compact, connected set with locally regular density. This satisfies the regularity conditions for being locally approximated by a smooth low-dimensional manifold $\mathcal{M}_k \subset R_k$.

Therefore, the dataset exhibits a *multi-manifold structure*, with each class associated to a well-separated, compact, structured region in \mathbb{R}^d .

Appendix C. Implementation Details

In this section, we present the prompts (manual templates) used by TextGrad for each dataset.

C.1 Prompt Design in TextGrad

For every task we compose a system prompt that fixes the global behaviour of GPT-4o and a task prompt that encodes the input variables.

The forward model receives the concatenation: <task-prompt> + <in-context demos> + <query>.

Confidence filter. A sample is kept in the loss only if

$$\max_c p_\theta(y = c \mid x) \geq 0.80$$

This threshold was tuned once on GLUE and reused everywhere else.

Hyper-parameters.

- Optimiser: TGD (step size 1.0, temperature 0.7);
- Prompt length cap: 256 GPT-4o tokens;
- Demonstrations per query: $K = 4$;
- PAPO iterations T : 10 (classification) / 5 (reasoning datasets).

C.2 Prompt Design for Each Task

Appendix D. Illustrative Example

In this section, we present the optimized prompts for the SimpleQA (Wei et al., 2024) dataset as an illustration.

Example of the SimpleQA dataset

Prompt at initialization:

You will answer a general-knowledge question on \$topic topic. Always conclude the last line of your response should be of the following format: 'Answer: \$VALUE' where VALUE is a \$answer_type value."

Prompt refined by PAPO:

You will answer a general-knowledge question. Restate the question in your own words to ensure understanding. Compare it with the examples provided above, note any shared entities and relations. Reason through the composition using evidence from both the question and demonstrations. Cross Check your conclusion, ensure it does not contradict any high confidence example. Always conclude the last line of your response should be of the following format: 'Answer: \$VALUE' where VALUE is a \$answer_type value."

Dataset	Initial prompt z_0
SST-2	Review: {sentence}, Options: {options}. Answer:
CoLA	Sentence: {sentence} Options: {options}. Answer:
MNLI	Premise: {premise}\nHypothesis: {hypothesis}\nOptions: {options}. Answer:
QQP	Question 1: {question1}\nQuestion 2: {question2}\nOptions: {options}. Answer:
MRPC	Sentence 1: {sentence1}\nSentence 2: {sentence2}\nOptions: {options}. Answer:
RTE	Premise: {sentence1}\nHypothesis: {sentence2}\nOptions: {options}. Answer:
WNLI	Sentence 1: {sentence1}\nSentence 2: {sentence2}\nOptions: {options}. Answer:
CAIS/MMLU	Question: {question}, Options: {options}. Answer:
SimpleQA	You will answer a general-knowledge question on \$topic topic. Always conclude the last line of your response should be of the following format: 'Answer: \$VALUE' where VALUE is a \$answer_type value."
GPQA	You will answer a professional knowledge question. Think step-by-step. Always finish with Answer: \$OPTION where OPTION is the letter of the correct choice.

Table 4: Initial prompt templates for all datasets evaluated in the paper.